

Interaction of Plum Pox Virus with Specific Colloidal Gold-Labeled Antibodies and Development of Immunochromatographic Assay of the Virus

N. A. Byzova^{1*}, I. V. Safenkova¹, S. N. Chirkov², V. G. Avdienko³, A. N. Guseva³,
I. V. Mitrofanova⁴, A. V. Zherdev¹, B. B. Dzantiev¹, and J. G. Atabekov²

¹*Bach Institute of Biochemistry, Russian Academy of Sciences, Leninsky pr. 33,
119071 Moscow, Russia; fax: (495) 954-2804; E-mail: nbyzova@inbi.ras.ru*

²*Faculty of Biology, Lomonosov Moscow State University, 119991 Moscow, Russia*

³*Central Scientific Research Institute of Tuberculosis, Russian Academy of Medical Sciences,
Yauzskaya Alley 2, 107564 Moscow, Russia*

⁴*Nikitsky Botanical Garden, National Scientific Center, Ukrainian Academy of Agrarian Sciences, 98648 Yalta, Ukraine*

Received June 23, 2010

Revision received July 16, 2010

Abstract—Two monoclonal antibodies (mABs) raised against plum pox virus (PPV) were shown to recognize its D, M, and C strains. Conjugates of the antibodies with colloidal gold (CG) nanoparticles averaging 26 nm in diameter were synthesized. The binding constants of PPV with both the native and conjugated mABs were determined using a Biacore X device. The complexes between the CG–mAB conjugates and plum pox virions were examined by means of transmission electron and atomic force microscopy. Using the conjugates with optimal component ratio, an express immunochromatographic assay of PPV was developed with a detection limit of 3 ng/ml and duration of 10 min. The assay was tested for PPV detection in samples of stone fruit tree leaves and demonstrated a good compatibility with the data obtained by “sandwich”-ELISA. The developed assay can be used in the field and applied for monitoring viral infection and for quarantine purposes.

DOI: 10.1134/S000629791011012X

Key words: plum pox virus, monoclonal antibodies, colloidal gold, transmission electron microscopy, atomic force microscopy, immunochromatographic assay

Plum pox virus (PPV; genus *Potyvirus*, family Potyviridae) is the most devastating pathogen of stone fruit trees. Plum pox virions are filamentous particles, 750 nm in length and 15 nm in diameter, composed of one molecule of RNA ((+)ssRNA) and protein envelope, the subunit having a molecular mass of 36-38 kDa [1]. At this time, six strains of the pathogen have been identified:

Dideron (D), Marcus (M), Cherry (C), El Amar (EA), Winona (W), and Rec (recombinant of D and M), differing in nucleotide sequence, antigen specificity, and epidemiological features [2].

PPV causes the sharka disease of cultivated and wild plants from the genus *Prunus*, such as plums, peaches, apricots, etc., which results in severely reduced fruit production because of premature fruit dropping and impairment of quality. The economic loss from this disease worldwide exceeded 10 billion Euros over the last 30 years, and the number of culled trees was in the millions [3]. Although PPV in most countries is a quarantine object, it is distributed in stone fruit orchards virtually worldwide [4]. As a rule, the virus populates a new region together with infected plants and is transmitted by aphids and by the transfer of infected plant material to new locations. The only way to manage the disease is to destroy all infected trees, so perfecting diagnostic strategies is of major importance.

Abbreviations: AB1, mAB clone 1D5B1; AB2, mAB clone 2H2F6; AFM, atomic force microscopy; CG, colloidal gold; ELISA, enzyme-linked immunosorbent assay; ICA, immunochromatographic assay; IgG, immunoglobulin G; mAB, monoclonal antibody; PBS, phosphate buffered saline (50 mM K⁺-phosphate buffer, pH 7.4, containing 0.1 M NaCl); PBST, PBS with 0.05% Tween 20; PBSTB, PBS containing 0.05% Tween 20 and 0.05% bovine serum albumin (BSA); PPV, plum pox virus; TEM, transmission electron microscopy.

* To whom correspondence should be addressed.

A series of sensitive serological and molecular methods for laboratory diagnostics of PPV have been developed to date [5, 6]; they are applied in accordance with diagnostic protocol [7] validated by the European and Mediterranean Plant Protection Organization (EPPO) to ensure reliable detection of the virus. The accuracy of sampling for laboratory analyses is crucial for efficacy of PPV detection in fruit tree orchards. Since characteristic symptoms of viral infection are not always observed, visual estimation of infection severity is not sufficient for the sampling. Accuracy of the sampling can be considerably increased by means of quick preliminary estimation of virus distribution among plants using the methods of field diagnostics. One of these methods is immunochromatographic assay (ICA) on test-strips, which is no less effective than enzyme-linked immunosorbent assay (ELISA) in identification of infected trees [8-12]. Immunochromatography is characterized by speed, sensitivity, and simplicity; the test has no requirement in additional equipment and reagents and in special professional skill. Because of their reliability, immunochromatographic tests are included in EPPO diagnostic protocols for determination of a number of phytopathogenic viruses [13, 14].

Recently, we were the first to develop an original Russian technology for production of test strips allowing detection of phytopathogenic viruses that uses polyclonal rabbit antibodies against viruses and nanoparticles of colloidal gold (CG) [15, 16]. These strips allow rapid (within 10 min) detection of morphologically distinct viruses, such as potato viruses X and Y, tobacco mosaic virus, bean mild mosaic virus, and carnation mottle virus. However, the polyclonal antibody-based test strips prepared according to this technology were ineffective for PPV diagnostics in stone fruit tree samples.

The goal of this work was to prepare and characterize monoclonal antibodies against PPV and to develop an immunochromatographic test with these antibodies, allowing rapid detection of this virus in fruit tree leaf samples.

MATERIALS AND METHODS

Chemicals. The following chemicals were used: goat (GAMIss), rabbit (RAMIss), and sheep (SAMIss) anti-mouse IgG antibodies (ABs) and sheep anti-rabbit IgG ABs (SARIss) (Imtek Bio, Russia); goat (Arista Biologicals, USA) and rabbit (DakoCytomation, Denmark) anti-mouse IgG ABs; bovine anti-mouse IgG ABs—horseradish peroxidase conjugate (Medgamal, Russia); Triton X-100, Tween 20, 3,3',5,5'-tetramethylbenzidine hydrochloride, sodium azide, polyvinylpyrrolidone ($M_r \sim 29$ kDa), and HEPES (Sigma, USA); hydrogen tetrachloroaurate(III) (Fluka, Germany); BSA, sodium citrate, Freund's incomplete adjuvant, and glycine (MP Biomedicals, UK); glycerol (Dia-M, Russia);

polyvinyl formal and tungsten phosphoric acid (SPI Supplies, USA); and surfactant P20 (Biacore AB, Sweden). All salts, acids, alkali, and organic solvents were of analytical or chemical purity grade.

Monoclonal antibodies were prepared using RPMI-1640 medium, fetal calf serum, HybriMax HAT-medium, HT-medium, mercaptoethanol, sodium pyruvate, penicillin, streptomycin, pristane, and Protein A-Sepharose CL-4B (Sigma). ELISA was carried out using Costar 9018 96-well transparent polystyrene plates (Corning Costar, USA). Solutions for synthesis of CG and its conjugates were prepared in MilliQ deionized water (Millipore, USA).

Isolation of PPV. PPV-NAT strain D was kindly provided by Prof. E. Maiss (Institute of Plant Diseases and Plant Protection, University of Hanover, Germany) [17]. The virus was propagated in tobacco (*Nicotiana benthamiana*) plants and purified as described elsewhere [18].

Preparation of monoclonal antibodies. Hybridomas producing ABs against PPV were prepared by fusion of BALB/c murine syngenic Sp2.0 line myeloma cells with immune BALB/c splenocytes using polyethylene glycol [19]. The immunization protocol included three fortnightly intraperitoneal injections of PPV (50 μ g per animal) in Freund's incomplete adjuvant mixture (1 : 1). The anti-PPV antibody titer in blood serum was determined by ELISA. Mice producing the highest titer were used for isolation of immune splenocytes.

Hybrid cells were grown at 37°C in an atmosphere containing 5% CO₂ in a CO₂-incubator (Queue, USA) in selective HAT-medium prepared on the base of commercial RPMI-1640 medium contained inactivated fetal calf serum (20%), 2-mercaptoethanol (5 μ M), sodium pyruvate (1 mM), penicillin (10 U/ml), streptomycin (10 U/ml), and HybriMax HAT-concentrate (1 : 50). After one week this medium was partially substituted with fresh medium, after two weeks it was completely substituted with HT-medium (HAT-medium without aminopterin), and after one month with medium containing all components but HAT-concentrate.

From 10th day of cell fusion, supernatants in the wells with apparent growth were tested for hybridomas producing anti-PPV ABs by indirect solid-phase ELISA. Selected monoclonal antibodies were propagated *in vitro* in 50-ml culture flasks and as ascitic tumors in the abdominal cavity of BALB/c mice injected intraperitoneally with 1 ml of pristane one week before injection of a monoclonal antibody [20]. Hybridomas taken for injection were suspended in 0.5-1.0 ml of RPMI-1640 ((1-4)·10⁶ cells per animal). Ten to twenty days after the beginning of ascites development, ascitic fluid was isolated. Antibodies were purified by affinity chromatography on Protein A-Sepharose CL-4B [21].

Determination of antibody titer by indirect solid-phase ELISA. PPV was sorbed in the wells of a 96-well plate overnight at 4°C from 100 μ l of solution containing

0.2 µg/ml of the virus in PBS (50 mM K⁺-phosphate buffer, pH 7.4, containing 0.1 M NaCl). The plate was washed four times with PBS containing 0.05% Tween 20 (PBST), and then serial dilutions of mABs (0.1 through 100 ng/ml; 100 µl per a well) in PBST were added and incubated at 37°C for 1 h. The plate was washed again, and 100 µl of anti-mouse immunoperoxidase conjugate (1 : 6000 in PBST) was added into each well and incubated at 37°C for 1 h. Following washing, the catalytic activity of immobilized enzyme was determined with peroxidase substrate 3,3',5,5'-tetramethylbenzidine (0.4 mM) and H₂O₂ (3 mM) dissolved in 40-mM Na⁺-citrate buffer, pH 4.0. The substrate solution was added to the plate wells (100 µl per well) and incubated in the dark at room temperature for 15 min. The reaction was terminated by addition of 50 µl of 1 M H₂SO₄, and optical absorbance of enzymatic reaction products was determined at 450 nm (*A*₄₅₀).

Characterization of colocation of PPV determinants recognized by monoclonal antibodies by ELISA. Analysis was carried out by comparison of binding dependencies on concentration of individual antibodies and their equimolar mixture [22]. PPV was sorbed in the plate wells from 100 µl of virus solution (0.2 µg/ml) in PBS overnight at 4°C. The plate was washed four times with PBST, and then serial dilutions of mABs or their equimolar mixture (0.1 through 50 ng/ml; 100 µl per well) in PBST were added and incubated at 37°C for 1 h. The plate was washed again, and 100 µl of anti-mouse immunoperoxidase conjugate (1 : 6000 in PBST) was added into each well and incubated at 37°C for 1 h. Following washing, immobilized peroxidase activity was determined as described above.

Preparation of colloidal gold by the citrate method [23]. One milliliter of 1% HAuCl₄ was added to 97.5 ml of deionized water, heated to boiling, and 1.5 ml of 1% sodium citrate was added on agitation. The mixture was boiled for 25 min, cooled, and stored at 4–6°C.

Preparation of mAB–CG conjugates. The choice of mAB concentration for conjugation between CG and mAB was made according to recommendations of Panerai et al. [24], implying determination of *A*₅₈₀ following addition of antibodies and 10% NaCl to the colloid. To do this, 1 ml of CG (*A*₅₂₀ = 1.0) was added to 0.1 ml of aqueous mAB solutions (concentration varied from 5 to 250 µg/ml), agitated, and incubated at room temperature for 10 min. Then, 0.1 ml of 10% NaCl was added to each sample, agitated, and following incubation for 10 min *A*₅₈₀ was determined. The concentration corresponding to the beginning of the plateau in the flocculation curve (a plot of *A*₅₈₀ versus concentration) was determined, and that exceeding this value by 10–15% was chosen for mAB conjugation.

Before conjugation with CG, antibodies were dialyzed against 1000 volumes of 10 mM sodium carbonate buffer, pH 9.5, at 4°C for 2 h. CG (*A*₅₂₀ = 1.0) was adjust-

ed with 0.1 M K₂CO₃ to pH 9.5, and then mAB solution of chosen concentration was added to the colloid. The mixture was incubated at room temperature for 45 min with continuous agitation followed by addition of BSA to the final concentration of 0.25%. CG particles with immobilized mABs were separated by centrifugation at 8000g for 30 min. The supernatant was removed, and the pellet was resuspended in PBS containing 0.05% BSA and 0.05% Tween 20 (PBSTB). When long storage was required, sodium aside (final concentration 0.02%) was added to the product.

Determination of binding constants for the interaction of PPV with mABs and mAB–CG conjugates. Equilibrium constants of immunochemical reactions were measured on a Biacore X system (Biacore AB). mABs dissolved in 10-mM Na⁺-citrate buffer, pH 5.0 (final concentration 50 µg/ml) were immobilized on the surface of a CM3 chip (Biacore AB). Then the following reagents were sequentially added into the cell: 5 µg/ml of PPV in HEPES-P buffer (Biacore AB); mAB at concentration of 4 through 400 nM (constants were calculated toward antibodies) or mAB–CG conjugate at concentration of 2 through 70 pM of CG (constants were calculated toward CG particles) in HEPES-P buffer (Biacore AB); HEPES-P buffer (10 mM HEPES, pH 7.4, containing 150 mM NaCl and 0.005% surfactant P20); and regenerating reagent (10 mM glycine-HCl, pH 2.0).

Measurements were carried out against a control cell, in which antibodies were not immobilized on the chip, and other reagents were the same as those in experimental cell. Constants were calculated using the BIAevaluation software (Biacore AB) in the steady-state affinity mode.

Transmission electron microscopy (TEM). Specimens of CG (*A*₅₂₀ = 1.0), mAB–CG conjugates (*A*₅₂₀ = 5.0, in PBSTB), and PPV (50 µg/ml in PBS) were placed onto copper TEM sample support grids (mesh 300; Pelco International, USA) covered with a film formed from polyvinyl formal solution in chloroform. Following sorption for 15 min, the specimens were washed with bidistilled water, negatively stained with 2% tungsten phosphoric acid for 1 min, and dried. For immune complex imaging, mAB–CG conjugate (*A*₅₂₀ = 5.0, in PBSTB) was added to the immobilized and washed PPV specimen, incubated for 15 min, washed with bidistilled water, counterstained as described above, and dried. Images were obtained on a CX-100 electron microscope (Jeol, Japan) at accelerating voltage 80 kV. Digital photos were analyzed using the UTHSCSA Image Tool software (UTHSCSA Dental Diagnostic Science, USA). The virus/antibody ratio in the immune complex was calculated from the average CG diameter and average distance between the conjugate particles adsorbed on the surface of a virion.

Atomic force microscopy (AFM). Specimens of PPV (100 µg/ml PBS) and mAB–CG conjugate (*A*₅₂₀ = 5.0, in

PBSTB) were placed on the surface of freshly cleaved mica (MICA V-1 GRADE, Cat. No. 1873-CA; SPI Supplies, USA), sorbed for 15 min (conjugate) or 5 min (PPV), washed with bidistilled water, and, after removal of excess water, dried. For immune complex imaging, mAB–CG conjugate was added to the immobilized and washed PPV specimen, incubated for 15 min at room temperature, washed with bidistilled water, and, after removal of excess water with filter paper, dried. Specimens were scanned on a SmartSPM atomic force microscope (AIST-NT, Russia) using fpN01HR cantilevers (Nanotuning, Russia) with a tip radius curvature of about 1 nm. The obtained images were analyzed using the Gwiddion software (Czech Metrology Institute, Czech Republic).

Development of immunochromatographic test systems. Test systems were assembled on mdi EasyPack membranes (Advanced Microdevices, India). Using an IsoFlow automated dispenser (Imagene Technology, USA), the mAB–CG conjugate diluted to $A_{520} = 2.0$ was applied onto the substrate (32 μ l per 1 cm of the strip). Anti-PPV mAB was used for formation of the test zone and IgG isolated from antiserum against mouse IgG for formation of the control zone. In both cases, 2 μ l of solution (0.5 mg/ml PBS containing 10% glycerol) were placed onto 1 cm of the strip. The mounted multimembrane composite was cut on an Index Cutter-1 (A-Point Technologies, USA) into strips, 78 \times 3.5 mm, which were hermetically packed into bags composed of laminated aluminum foil and containing silica gel as desiccant, using an FR-900 continuous band sealer (Wenzhou Dingli Packing Machinery, China). Cutting and packing were carried out at 20–22°C in a separate room with relative humidity no more than 30%.

Immunochromatographic assay. The assay was carried out at room temperature. The sample pad of the test strip kept vertically was dipped in the analyzed sample for 1.5 min, taken out, and placed onto a horizontal surface. Result of analysis was determined in two interchangeable ways: digital imaging of the test strip on a BearPaw 4800TA Pro scanner (Mustek, Taiwan) with calculation of integrated intensity of colored zones using the TotalLab software or using a Reflecom system (Okta-Medika, Russia) performing digital image capture and analysis [25].

Plant sampling. Leaves of plum (*Prunus domestica*), myrobalan (*P. cerasifera*), peach (*P. persica*), and apricot (*P. armeniaca*) manifesting symptoms of viral infection, as well as asymptomatic leaves were collected according to the approved protocol [7] in June and September, 2008–2009, at orchards of stone fruit trees disposed in Southern Coast, piedmont, and prairie zones of Crimea, Ukraine.

Testing of plant samples by ELISA. The testing was carried out using an ELISA Reagent Set, Cat. No. SRA 31505 (Agdia, USA), according to the manufacturer's

protocol. This set identified all of the known virus strains. Extract from the *N. benthamiana* leaves infected by PPV was used as positive control. Extracts from healthy plum, peach, myrobalan, and apricot leaves served as negative controls. Optical absorbance of enzymatic reaction products (A_{405}) was determined on a Multiscan Plus vertical photometer (Labsystems, Finland).

Strain specificity of identified PPV isolates. Strain specificity was determined using PPV Dideron (Cat. No. K-12B), PPV Marcus (K-11B), PPV Cherry (K-14B), and PPV El Amar (K-13B) diagnostic kits (Agritest, Italy), containing mABs specific to the strains D, M, C, and EA, respectively. Both positive (strain-specific) and negative controls are components of these kits. Analyses were performed according to the manufacturer's protocols.

Strain specificity of mABs raised in this work. It was determined using the same kits (Agritest), in which mABs specific to D, M, or C strain were replaced by either AB1 or AB2 antibodies at 1.5 μ g/ml concentration. Subsequently, their interaction with positive controls of D, M, and C strains was tested.

Plant specimen preparation for ICA. A leaf piece, 150–170 mg wet weight, was placed into a polyethylene bag with enclosed plastic net (mesh size 2 \times 2 mm), and 3 ml of extracting buffer (PBS containing 0.1% Tween 20, 0.5% Triton X-100, and 1% polyvinylpyrrolidone ($M_r \sim 29$ kDa)) was added. The bag was put on hard surface, and the leaf fragment was kneaded for 30 sec. The content of the bag was mixed up by rocking motion and transferred into a tube.

RESULTS AND DISCUSSION

Characterization of anti-PPV mABs. A series of clones producing antibodies against PPV was raised as a result of hybridization. Two monoclonal antibodies were selected for further work: 1D5B1 (AB1) and 2H2F6 (AB2). Specific binding of these antibodies with the standard antigen specimen was detected at low concentrations (<0.5 ng/ml) in indirect ELISA.

The use of these antibodies in serological tests implies relative positioning of the recognized epitopes. The data of comparing concentration dependencies for individual AB1 and AB2 clones and their equimolar mixture are given on the Fig. 1. Titration of the mAB equimolar mixture (curve 3) compared with individual mABs (curves 1 and 2) showed higher signal, which, however, was less than the theoretically calculated sum of individual signals (dashed curve). These data suggest that AB1 and AB2 interact with different epitopes of the viral envelope protein that are localized nearby or partly overlap each other.

Association constant measurements for the interaction of the prepared mABs with PPV using Biacore X

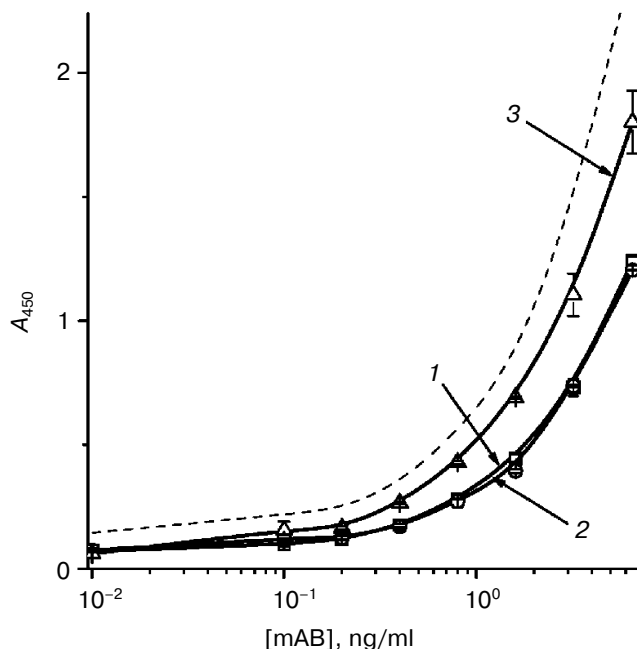


Fig. 1. Plot of AB1 (1), AB2 (2), and their equimolar mixture (3) binding with immobilized PPV against concentration, as evaluated by ELISA. The dashed line shows the sum of curves 1 and 2.

equipment demonstrated close values of these constants: $6.9 \cdot 10^7 \text{ M}^{-1}$ (AB1) and $5.8 \cdot 10^7 \text{ M}^{-1}$ (AB2) (Fig. 2, a and b).

The data on strain specificity of AB1 and AB2 given in Table 1 demonstrate that both mABs interact with three PPV strains at the level comparable with that of commercial monoclonal antibody. While AB1 recognizes PPV isolates belonging to the strains M and D, AB2 more effectively recognizes strain C.

Characterized mABs were used for development of immunochromatographic test systems for PPV detection.

Characterization of CG specimen by TEM. A specimen of CG was synthesized for the use as a label. The size

of prepared CG particles (Fig. 3) was as follows (mean size \pm standard deviation): long axis = $30 \pm 7 \text{ nm}$; short axis = $22 \pm 5 \text{ nm}$; and ellipticity (axial ratio) = 1.3 ± 0.2 . These data suggest high homogeneity of the CG specimen.

Preparation of mAB–CG conjugates. Figure 4 shows the plot of A_{580} of mAB–CG conjugate solutions versus mAB concentration in the presence of 10% NaCl. One can see that addition of antibodies initially results in elevation of absorbance, followed by decrease of A_{580} value and its reaching a plateau. As a rule [24], the antibody concentration exceeding the point of reaching the plateau by 10–15%, which corresponds to formation of stable non-aggregating conjugates, is taken as optimal for conjugation. According to these recommendations, $10 \mu\text{g/ml}$ concentration was chosen for AB1 and $16 \mu\text{g/ml}$ for AB2.

Characterization of immune complexes between PPV and mAB–CG by AFM and TEM. Visualization of immune complexes by TEM using negative counterstaining (Fig. 5) showed that the particles of mAB–CG conjugate are localized at periphery of virions, and their area density depends on both CG size and concentration of interacting reagents. Minimal distance between adjacent CG particles immobilized on the PPV surface is 3.5 nm, maximum (which does not exceed the CG particle size) 28.8 nm, and the average distance between CG particles is 11.4 nm. The latter distance probably corresponds to the space occupied by antibodies bound with colloidal particles.

The immune complex images obtained by AFM (Fig. 6) correspond to both morphology of virions and conjugate sizes determined by TEM. The height of virion on the profile of the AFM image (Fig. 6b) is 12 nm corresponding to 12.5–13.0 nm on the data of TEM (Fig. 5). This parameter also corresponds to the data from the ICTV (International Committee on Taxonomy of Viruses) database, in which the PPV diameter is estimat-

Table 1. Comparative reactivity of AB1 and AB2 to various PPV strains in indirect “sandwich” ELISA

PPV strain	Absorbance of enzymatic reaction products				
	Strain specificity of Agritest diagnostic kit			mABs, 1.5 $\mu\text{g/ml}$	
	D	M	C	AB1	AB2
D	1.293	0.083	0.105	1.925	0.803
M	0.081	2.046	0.080	2.613	0.932
C	0.094	0.099	0.874	0.391	0.880
Negative control	0.083	0.108	0.130	0.113	0.135

Note: Positive controls comprising the Agritest diagnostic kits served as a source of strains D, M, and C. Negative control was from the same kits. Data of typical experiment are presented.

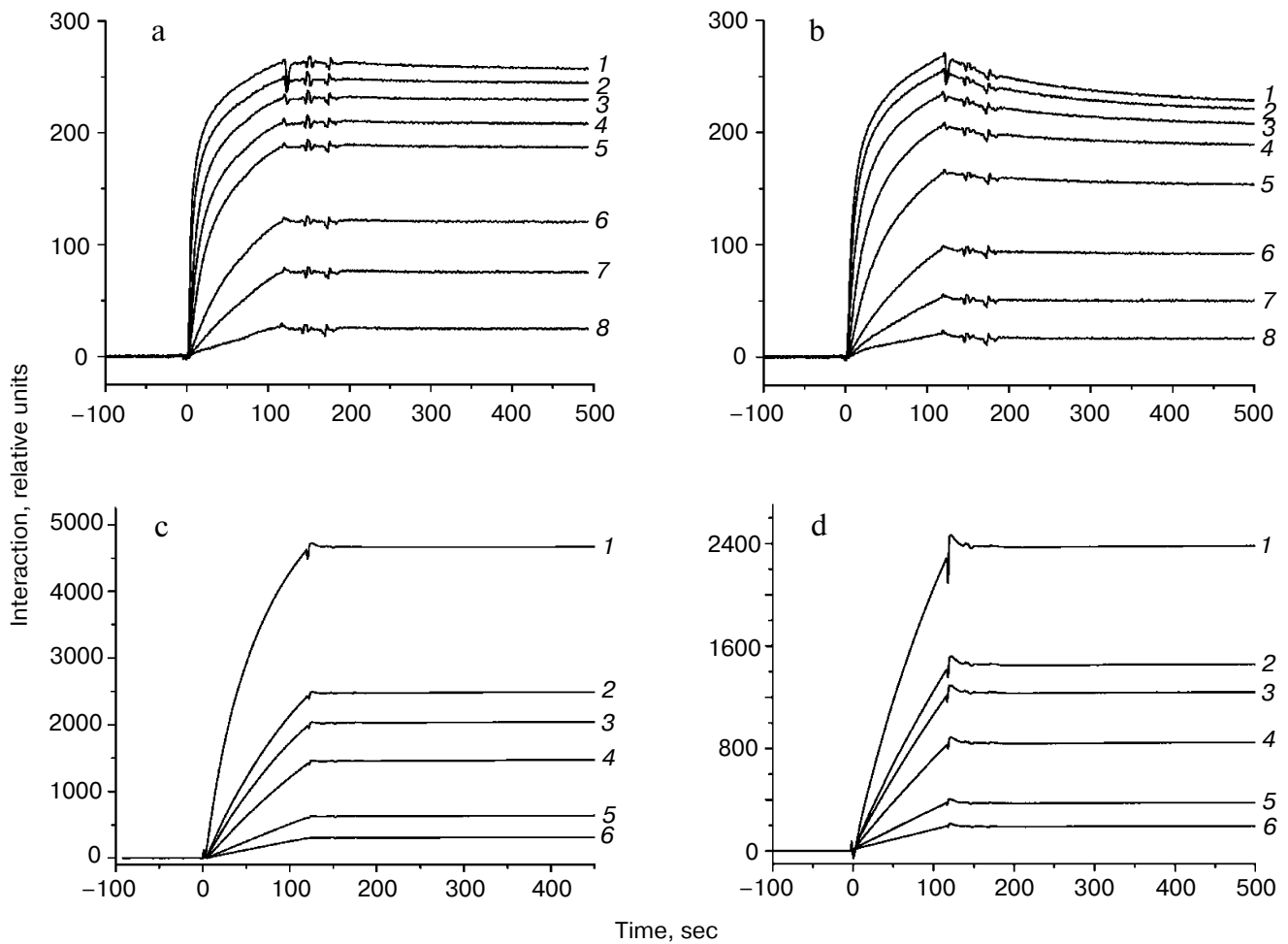


Fig. 2. Kinetics of PPV interaction with mABs determined using a Biacore X system. a) AB1; b) AB2; c) AB1–CG conjugate; d) AB2–CG conjugate. a, b: 1–8) Concentrations of the added antibodies were 400, 200, 100, 60, 30, 10, 8, and 4 nM, respectively. c, d: 1–6) Concentrations of the added conjugates given in optical density units at 520 nm were 3, 1, 0.8, 0.5, 0.2, and 0.1, respectively.

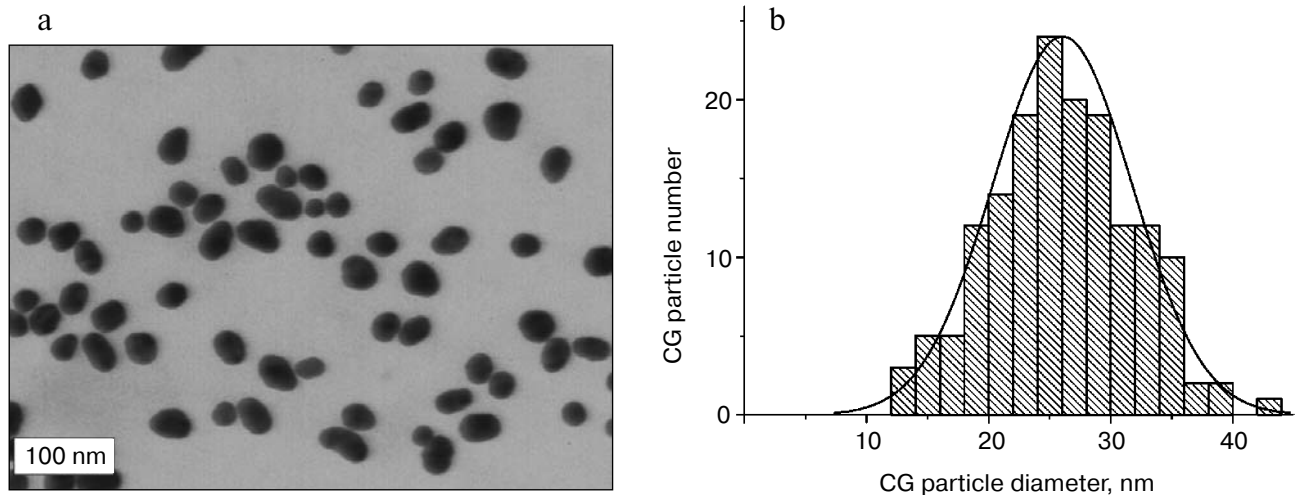


Fig. 3. TEM image of CG specimen (a), and size distribution of CG particles (b). The mean size is 26 nm, and the standard deviation is 6 nm ($n = 160$).

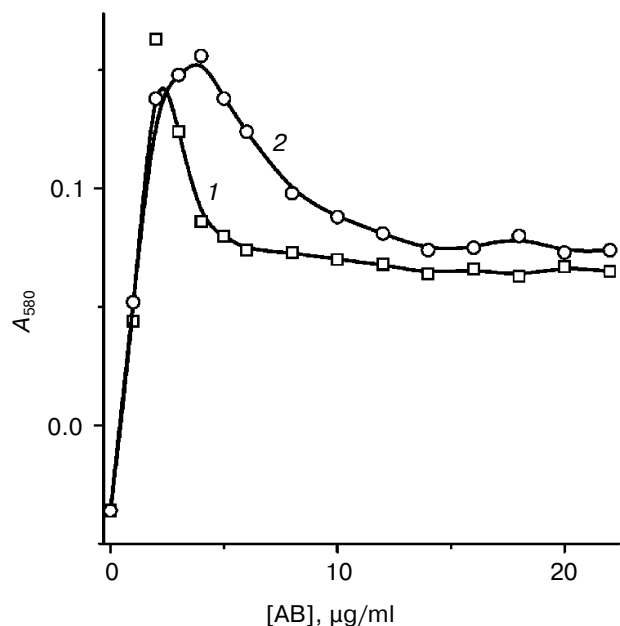


Fig. 4. Flocculation curves of anti-PPV mAB immobilization (AB1 (1); AB2 (2)) on CG particles. Zero level of A_{580} corresponds to CG in absence of both antibodies and NaCl.

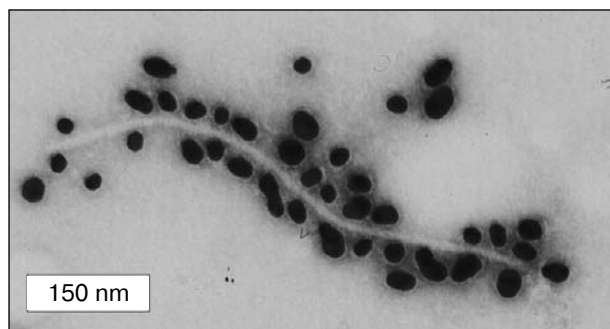
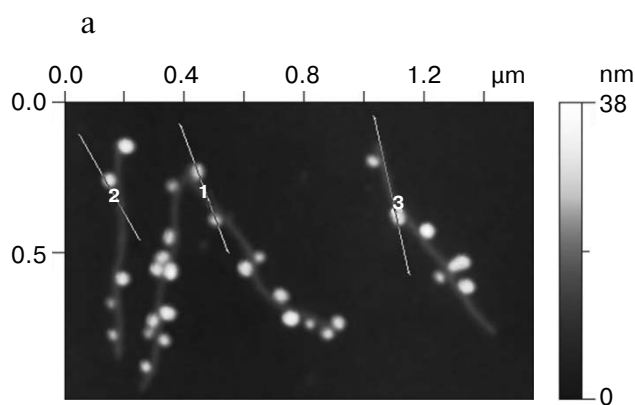


Fig. 5. TEM image of complexes between PPV and AB1-CG conjugate particles.



ed as 12.5 to 20 nm. Note that AFM allows visualization of conjugates disposed above the viral particles lying on the underlying surface.

The structure of PPV – with its regularly repeating epitopes on the surface – determines formation of complexes with mAB–CG conjugates with virus/conjugate ratios up to 1 : 37 (an example of PPV complex with AB1–CG conjugate is shown in Fig. 6).

Quantitative characterization of interaction between PPV and mAB–CG on a Biacore X device. The obtained dependencies for conjugates of CG with AB1 and AB2 are shown on the Fig. 2, c and d. Association constants were $1.9 \cdot 10^{10} \text{ M}^{-1}$ for AB1–CG and $1.4 \cdot 10^{10} \text{ M}^{-1}$ for AB2–CG. Equilibrium constants were calculated for free antibodies or AB-conjugated CG particles. Taking in account that synthesis of mAB–CG conjugate according to the protocol described in “Materials and Methods” gives the number of antibody molecules immobilized on the CG particle, which is close to the S_{CG}/S_{AB} ratio, where S_{CG} is the surface of CG particle and S_{AB} is the surface of antibody molecule (45 nm^2 [26]). This gives about 50 AB molecules per CG particle, $\sim 26 \text{ nm}$ in diameter. Thus, variation of equilibrium constant on transition from antibodies to conjugates is probably explained by elevation in number of binding centers in immune complexes due to consolidation of several AB molecules on one CG particle (Table 2). Several orders increase (depending on size of colloidal carrier) in affinity of anti-PPV conjugates compared with initial antibodies was reported earlier [27].

Development of immunochromatographic test system for detection of PPV. Since viruses are polyvalent antigens, maximum sensitivity of their detection [28] is achieved using “sandwich” ICA (Scheme). The analyzed sample is adsorbed in the sample zone of the test strip (Scheme, 2). PPV, if presented in the sample, interacts with specific mAB (Scheme, a) labeled with colloidal gold (Scheme, b) and localized in the starting zone of the test strip (Scheme, 3). The formed antigen–antibody

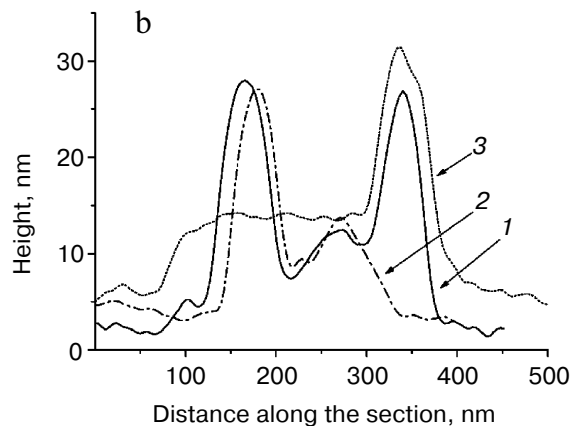
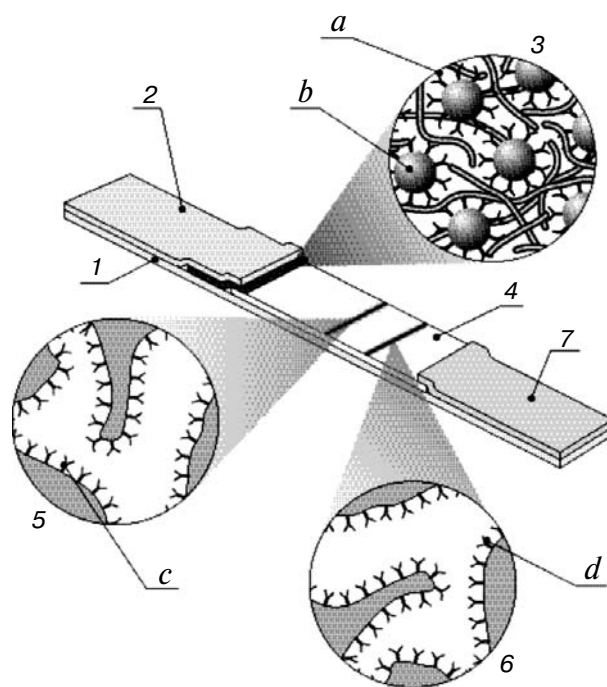


Fig. 6. Atomic force microscopy of complexes between PPV and AB1–CG conjugate particles. a) Image of complexes with marked sections. Curves 1–3 correspond to sections along which particle sizes were determined; b) profiles of sections 1–3.

complex interacts with anti-PPV mAB (Scheme, *c*) immobilized in the test zone (Scheme, 5). Thus, appearance of a colored band in the test zone indicates a positive result of the test. When the sample does not contain PPV, this zone remains blank (negative result of the test). The control zone (Scheme, 6) contains ABs against murine IgG (Scheme, *d*), so the colored complex (immobilized ABs–mAB–CG) is formed in this zone independently of the presence of PPV in the tested sample.

We optimized this test system with the aim to achieve minimal threshold of PPV detection, obtain clear and intensely colored test and control zones, and minimize background. We compared four variants of “sandwich” ICA differing in anti-PPV mAB (AB1 or AB2) immobilized in the test zone and that conjugated with CG. The best result in amplitude of signal and detection threshold was achieved when AB1 was immobilized in the test zone and AB2–CG conjugate moved along the membrane. Maximum intensity of the test zone coloring was achieved when mAB solution with concentration of 0.5 mg/ml was used for immobilization on the membrane. Further increase of mAB concentration did not result in increase in intensity. The AB2–CG conjugate was applied onto a fiberglass membrane from a solution with $A_{520} = 2.0$, because the color intensity of both working zones reaches a plateau at this concentration [16].

Various species-specific anti-mouse IgG antibodies provided by different companies were used for the control zone formation. The data on binding of mAB–CG conjugates ($A_{520} = 2.0$) with different anti-mouse IgG antibodies (taken at concentration of 0.5 mg/ml for sorp-



Immunochromatographic “sandwich” assay. Test strip: 1) plastic base; 2) sample pad; 3) gold conjugate pad; 4) working membrane; 5) test zone; 6) control zone; 7) terminal adsorbing pad. Reagents: *a*) mAB–CG conjugate specific to PPV; *b*) CG particles; *c*) anti-PPV mAB immobilized in test zone; *d*) anti-species ABs immobilized in control zone

tion on the membrane) are shown in Table 3. Maximum binding of colloidal conjugate was attained with goat anti-mouse IgG antibodies (GAMI) from Arista Biologicals.

Characterization of immunochromatographic test system for detection of PPV. On the basis of the data of optimization, we prepared immunochromatographic test strips and tested the detection of PPV. Analytical features of the method were evaluated in a model using a purified PPV specimen added (up to a preset concentration) into extracting buffer or into the non-infected tobacco (*N. benthamiana*) leaf extracts, either clarified by low-speed centrifugation or unclarified.

Table 2. Association constants, M^{-1} , of interaction between PPV and mABs or their conjugates with CG

Specimen	AB1	AB2
Native mAB*	$6.9 \cdot 10^7$	$5.8 \cdot 10^7$
mAB–CG conjugate**	$1.9 \cdot 10^{10}$	$1.4 \cdot 10^{10}$

* Constants are calculated towards antibody.

** Constants are calculated towards AB-coated CG particle.

Table 3. Binding of various immobilized species-specific anti-mouse IgG antibodies with anti-PPV mAB–CG conjugates in the immunochromatographic system

Conjugated mAB	Color intensity of binding zone, arbitrary units					
	GAMIss (Imtek Bio)	RAMIss (Imtek Bio)	SAMIss (Imtek Bio)	GAMI (Arista Biologicals)	RAMI (DakoCytomation)	SARIss (Imtek Bio)
AB1	71	34	98	131	100	0
AB2	100	62	127	154	121	0

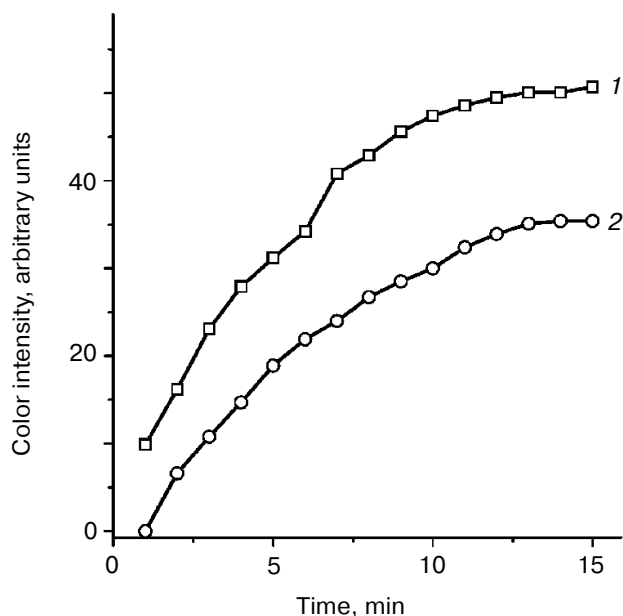


Fig. 7. Staining kinetics of control (curve 1) and test (curve 2) zones in immunochromatographic detection of PPV in unclarified extract of infected leaves of plum cultivar Kleimen.

Extracts from stone fruit leaves compared to those from herbaceous plants have remarkably higher viscosity. Hence, the test strips were tested for virus detection in leaf extracts of stone fruit plants infected with PPV. Mobility of the fluid front was found to vary depending on plant species and cultivar, but in all samples the front achieved the terminal absorbing pad within 5 min after submerging the test strip into the extract. Intensity of stained bands both in test and control zones achieved

maximum 10-15 min after dipping the sample pad of the test strip into the sample (Fig. 7). Hence, 10 min is the recommended time range for the assay.

Figure 8a shows the appearance of bands after the analysis, and Fig. 8b shows the dependence of staining intensity in test zone on PPV concentration in unclarified sample. Thus, the test strips enable PPV detection within 3 to 1000 ng/ml concentration range. Measurement error in determination of PPV concentration almost did not differ and varied from 5 to 10% in buffer and clarified and unclarified leaf extracts ($n = 4$).

Immunochromatographic test system testing. Eighteen samples of leaves manifesting disease symptoms and 11 asymptomatic samples of various stone fruits were collected and tested using an Agdia ELISA-based test system. PPV was detected in six samples manifesting symptoms, whereas the virus was absent in another 12 samples with symptoms and 11 asymptomatic samples. This data demonstrates unreliability of sampling on the basis of symptoms only and need to use analytical diagnostic methods for revealing infected plants. Analysis of positive samples using the Agritest strain-specific ELISA attributed all revealed isolates to the D strain (Table 4). The M, C, and EA strains were not revealed in the infected samples (data not shown).

All infected samples and four negative samples, one per each stone fruit species, were used for a comparison of efficacy of infected plant detection by ICA and ELISA. The data presented in Table 4 demonstrate equal efficacy using these two methods. The absence of staining in the test zone of the test strip, when analyzing uninfected sample, suggests specificity of the developed immunochromatographic method of PPV detection.

Thus, the proposed immunochromatographic mAB-based test system allows reliable detection of PPV in stone

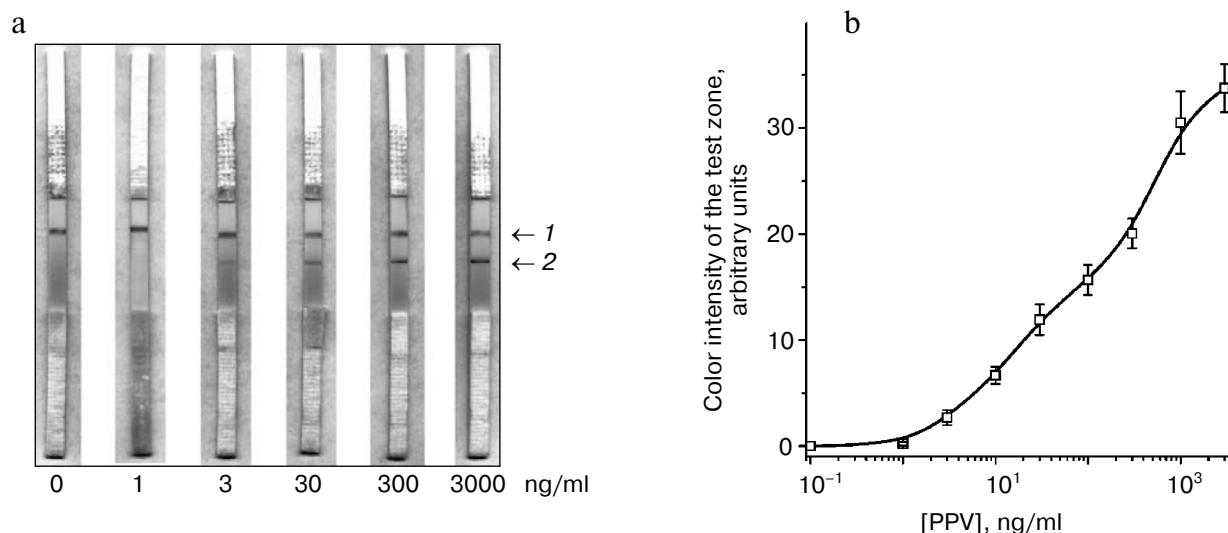


Fig. 8. Immunochromatographic detection of PPV in unclarified tobacco (*N. benthamiana*) leaf extract with added PPV specimen. a) Appearance of strips after the test (control zone (1); test zone (2)); b) dependence of color intensity of the test zone on PPV concentration.

Table 4. Detection of PPV in stone fruit samples by ICA and ELISA

Sample	Color intensity of test zone, arbitrary units	Agdia test system	Agritest test system specific to D strain
	ICA	ELISA	
Rootstock growth of myrobalan	15	1.090	1.506
Izum Erick plum	23	1.420	1.623
Kleimen plum	53	1.754	0.799
Peach T-IV 3/4	22	1.478	1.567
Nectarine	20	0.574	0.222
Purpurovaya myrobalan	5	1.263	0.338
Vilora myrobalan	< 1	0.043	0.079
October Sun plum	< 1	0.045	0.032
Markuleshti apricot	< 1	0.055	0.066
Ornamental peach	< 1	0.027	0.027

fruit leaf extracts within 10 min and can be used for analyses outside a laboratory, including field conditions. Extended testing and use of these tests by plant breeders and quarantine services can assist PPV monitoring, early detection of infection foci and sources, and more successful prevention of the virus spreading. It is important that the obtained AB1 and AB2 specifically react with several PPV strains. Their reactivity against M and D, the most widespread PPV strains, is experimentally demonstrated. Moreover, since the viral coat proteins of M and Rec strains are identical [29], this indicates the capability of detecting PPV isolates of Rec strain by ICA developed on the basis of these antibodies. Reactivity of these antibodies against the W strain is to be determined. This task is important because the W strain is supposed to originate from orchards of stone fruits in Ukraine [30] and, hence, can be present in contiguous territory of the Russian Federation.

Another important result of the work is the new proof of PPV presence in Crimea. The PPV geographical spread and strain variety is under intensive study due to its great economic importance [3]. The virus spread in orchards of stone fruits in Crimean territory was not studied to date, although typical symptoms of plum pox were repeatedly detected by visual inspection of the orchards

[31]. These observations were proved several times by the ELISA method [32]. In the present work, the presence of PPV in various areas of Crimea is verified using Agdia and Agritest test systems recommended by EPPO diagnostic protocol and enabling revelation of all known viral strains, as well as using the newly developed immunochromatographic test system for plum pox detection.

This study was supported by the Russian Foundation for Basic Research (grant No. 09-03-90412-Ukr_f_a), Federal Target Program "Scientific and Scientific-Pedagogical Personnel of Innovative Russia 2009-2013" (State contract No. P975 from August 20, 2009), and the Russian Academy of Sciences Fundamental Research Program "Fundamentals of Nanotechnologies and Nanomaterials".

REFERENCES

1. Salvador, B., Garcia, J. A., and Simon-Mateo, C. (2006) *EPPO Bull.*, **36**, 229-238.
2. Candresse, T., and Cambra, M. (2006) *EPPO Bull.*, **36**, 239-246.
3. Cambra, M., Capote, N., Myrta, A., and Llacer, G. (2006) *EPPO Bull.*, **36**, 202-204.
4. Glasa, M., and Candresse, T. (2005) *Plum Pox Virus. AAB Descriptions of Plant Viruses*, **410**, 1-12.
5. Cambra, M., Boscia, D., Myrta, A., Palkovics, L., Navratil, M., Barba, M., Gorris, M. T., and Capote, N. (2006) *EPPO Bull.*, **36**, 254-261.
6. Olmos, A., Capote, N., and Candresse, T. (2006) *EPPO Bull.*, **36**, 262-266.
7. Diagnostic Protocols for Regulated Pests. Plum Pox Potyvirus (2004) *EPPO Bull.*, **34**, 247-256.
8. Danks, C., and Barker, I. (2000) *EPPO Bull.*, **30**, 421-426.
9. Salomone, A., and Roggero, P. (2002) *J. Plant Pathol.*, **84**, 65-68.
10. Salomone, A., Bruzzone, C., Minuto, G., Minuto, A., and Roggero, P. (2002) *J. Plant Pathol.*, **84**, 193.
11. Salomone, A., Mongelli, M., Roggero, P., and Boscia, D. (2004) *J. Plant Pathol.*, **86**, 43-48.
12. Kusano, N., Hirashima, K., Kuwahara, M., Narahara, K., Imamura, T., Mimori, T., Nakahira, K., and Torii, K. (2007) *J. Gen. Plant Pathol.*, **73**, 66-71.
13. Diagnostic Protocols for Regulated Pests. Tomato Spotted Wilt Tospovirus, Impatiens Necrotic Spot Tospovirus and Watermelon Silver Mottle Tospovirus (2004) *EPPO Bull.*, **34**, 271-279.
14. Diagnostic Protocols for Regulated Pests. Beet Necrotic Yellow Vein Virus (Benyvirus) (2006) *EPPO Bull.*, **36**, 429-440.
15. Safenkova, I. V., Byzova, N. A., Chirkov, S. N., Blintsov, A. N., Zherdev, A. V., Dzantiev, B. B., and Atabekov, I. G. (2008) *Proc. All-Russ. Conf. "Chemical Analysis"*, Moscow, pp. 77-79.
16. Byzova, N. A., Safenkova, I. V., Chirkov, S. N., Zherdev, A. V., Blintsov, A. N., Dzantiev, B. B., and Atabekov, I. G. (2009) *Appl. Biochem. Microbiol.*, **45**, 204-209.

17. Maiss, E., Timpe, U., Briske, A., Jelkmann, W., Casper, R., Himmler, G., Mattanovich, D., and Katinger, H. W. (1989) *J. Gen. Virol.*, **70**, 513-524.
18. Lain, S., Riechmann, J. L., Mendez, E., and Garcia, J. A. (1988) *Virus Res.*, **10**, 325-342.
19. Shulman, M., Wilde, C. D., and Kohler, G. (1978) *Nature*, **276**, 269-270.
20. Moser, H., and Vecchio, G. (1967) *Experientia*, **23**, 1-10.
21. Lindmark, R., Thoren-Tolling, K., and Sjoquist, J. (1983) *J. Immunol. Meth.*, **62**, 1-13.
22. Wurzner, R., and Baumgarten, H. (1992) in *Monoclonal Antibodies* (Peters, J. H., and Baumgarten, H., eds.) Springer, Berlin, pp. 139-148.
23. Frens, G. (1973) *Nature Phys. Sci.*, **241**, 20-22.
24. Panerai, R. B., Chacon, M., Pereira, R., and Evans, D. H. (2004) *Med. Eng. Phys.*, **26**, 43-52.
25. Dzantiev, B. B., Zherdev, A. V., Popov, V. O., Vengerov, Yu. Yu., Starovoitova, T. A., and Toguzov, R. T. (2002) *Klin. Lab. Diagn.*, **8**, 25-31 [in Russ.].
26. Harris, L. J., Skaletsky, E., and McPherson, A. (1998) *J. Mol. Biol.*, **275**, 861-872.
27. Safenkova, I. V., Zherdev, A. V., and Dzantiev, B. B. (2010) *J. Immunol. Meth.*, **357**, 17-25.
28. Egorov, A. M., Osipov, A. P., Dzantiev, B. B., and Gavrilova, E. M. (1991) *Theory and Practice of Enzyme-Linked Immunoassay* [in Russian], Vysshaya Shkola, Moscow.
29. Glasa, M., Marie-Jeanne, V., Labonne, G., Subr, Z., Kudela, O., and Quiot, J. B. (2002) *Eur. J. Plant Pathol.*, **108**, 843-853.
30. James, D., Vagra, A., Thompson, D., and Hayes, S. (2003) *Plant Dis.*, **87**, 1119-1124.
31. Mitrofanova, O. V., Mitrofanova, I. V., Ezhov, V. N., Lesnikova-Sedoshenko, N. P., Lukicheva, L. A., Smykov, A. V., Senin, V. V., and Litvinova, T. V. (2005) *Bull. Nikitsky Bot. Garden*, **91**, 111-120 [in Russ.].
32. Mitrofanova, O. V., Mitrofanova, I. V., Chirkov, S. N., Ezhov, V. N., and Lesnikova-Sedoshenko, N. P. (2009) *Trudy Nikitsky Bot. Garden*, **131**, 94-103 [in Russ.].